The EMBO Journal (2009) 28, 3549–3563 | © 2009 European Molecular Biology Organization | All Rights Reserved 0261-4189/09
www.embojournal.org

THE EMBO JOURNAL

The MRT-1 nuclease is required for DNA crosslink repair and telomerase activity *in vivo* in *Caenorhabditis elegans*

Bettina Meier[1,2], Louise J Barber[3], Yan Liu[1], Ludmila Shtessel[1], Simon J Boulton[3], Anton Gartner[2,5] and Shawn Ahmed[1,4,5,*]

[1]Department of Genetics, University of North Carolina, Chapel Hill, NC, USA, [2]Wellcome Trust Centre for Gene Regulation and Expression, University of Dundee, Dundee, UK, [3]DNA Damage Response Laboratory, Cancer Research UK, Clare Hall Laboratories, South Mimms, UK and [4]Department of Biology, University of North Carolina, Chapel Hill, NC, USA

The telomerase reverse transcriptase adds *de novo* DNA repeats to chromosome termini. Here we define *Caenorhabditis elegans* MRT-1 as a novel factor required for telomerase-mediated telomere replication and the DNA-damage response. MRT-1 is composed of an N-terminal domain homologous to the second OB-fold of POT1 telomere-binding proteins and a C-terminal SNM1 family nuclease domain, which confer single-strand DNA-binding and processive 3′-to-5′ exonuclease activity, respectively. Furthermore, telomerase activity *in vivo* depends on a functional MRT-1 OB-fold. We show that MRT-1 acts in the same telomere replication pathway as telomerase and the 9-1-1 DNA-damage response complex. MRT-1 is dispensable for DNA double-strand break repair, but functions with the 9-1-1 complex to promote DNA interstrand cross-link (ICL) repair. Our data reveal MRT-1 as a dual-domain protein required for telomerase function and ICL repair, which raises the possibility that telomeres and ICL lesions may share a common feature that plays a critical role in *de novo* telomere repeat addition.

The EMBO Journal (2009) **28,** 3549–3563. doi:10.1038/emboj.2009.278; Published online 24 September 2009
Subject Categories: genome stability & dynamics
Keywords: *C. elegans*; ICL; POT1; SNM1; telomerase

Introduction

The ends of linear chromosomes, telomeres, pose two major challenges to the maintenance of chromosome integrity and overall genome stability: telomeres need to be adequately replicated, to compensate for the inability of canonical DNA polymerases to replicate the chromosome terminus, and they need to be protected from being mistakenly sensed and repaired as DNA double-strand breaks (DSBs).

Telomeric DNA is composed of simple, repetitive sequences. The 5′-to-3′ telomeric DNA strand is G-rich and terminates as a 3′ single-stranded overhang. Telomeric repeats are replenished by telomerase, a ribonucleoprotein composed of the telomerase reverse transcriptase (TERT) and an RNA component (TR) containing the telomere-repeat template (Greider and Blackburn, 1989; Collins, 2006). The catalytic subunit of telomerase, TERT, and its RNA component are sufficient to confer telomere-repeat addition *in vitro*. Additional proteins, many of which are essential, facilitate processing of TR and telomerase holoenzyme function (Collins, 2006; Fu and Collins, 2007; Venteicher *et al*, 2008). Mutations in the essential proteins dyskerin, NOP10, NHP2, as well as in TR and TERT, confer shortened telomeres and reduced *in vitro* telomerase activity in patients with heritable forms of Dyskeratosis Congenita and Pulmonary Fibrosis (reviewed by Vulliamy and Dokal, 2008). Thus, telomere maintenance defects can limit proliferation of cells in lymphatic or pulmonary systems *in vivo*, consistent with evidence that telomerase can limit the proliferative lifespan of human primary cells *in vitro* (Garcia *et al*, 2007).

Double mutants deficient for fission or budding yeast DNA-damage sensor proteins ATM and ATR display progressive telomere erosion, suggesting that DNA-damage signalling may be required for telomerase-mediated telomere maintenance *in vivo* (Naito *et al*, 1998; Ritchie *et al*, 1999; Nakamura *et al*, 2002). Conceptually related results were reported for *Caenorhabditis elegans* DNA-damage response mutants, where telomerase-mediated telomere replication was abolished *in vivo* by single mutations in subunits of the Rad9-Rad1-Hus1 (9-1-1) PCNA-like sliding clamp, *mrt-2* (the worm *rad1*) or *hus-1*, or its large RFC clamp loader subunit, *hpr-17* (Ahmed and Hodgkin, 2000; Hofmann *et al*, 2002; Boerckel *et al*, 2007). Further, subunits of the homologous mammalian 9-1-1 complex, as well as its RFC clamp loader, RAD17, were shown to physically interact with the telomerase holoenzyme, to bind to telomeric DNA *in vivo*, and to facilitate telomerase activity *in vitro* (Francia *et al*, 2006). However, knockdown of these mammalian DNA-damage response proteins is cell-lethal and results in dramatic, rapid effects on telomere length, precluding analysis of effects on telomerase-mediated telomere length maintenance *in vivo* (Francia *et al*, 2006). The former results suggest that DNA-damage response proteins may function at chromosome ends as a prerequisite for telomere repeat addition by telomerase. These proteins can respond to DSBs (d'Adda di Fagagna *et al*, 2004), suggesting that telomeres may be sensed as 'aberrant' DSBs when they are replicated during S-phase and that the 9-1-1 complex in conjunction with its clamp loader may facilitate recruitment of telomerase to chromosome termini.

Here we identify *C. elegans* MRT-1 as a novel factor required for *in vivo* telomerase activity. MRT-1 encodes a dual-domain protein with an N-terminus homologous to the second OB DNA-binding fold found in POT1 (Protection Of Telomeres 1) proteins and a C-terminus bearing homology to

*Corresponding author. Department of Genetics, University of North Carolina, Coker Hall, Chapel Hill, NC 27599-3280, USA.
Tel.: +1 919 843 4780; Fax: +1 919 962 4296;
E-mail: shawn@med.unc.edu
[5]These authors contributed equally as senior authors to this work

Received: 10 November 2008; accepted: 24 August 2009; published online: 24 September 2009

Table I Progressive brood size reduction and loss of viability in late generation *mrt-1*, *mrt-2* and *trt-1* mutants

	Generation												
	F2	F4	F6	F8	F10	F12	F14	F16	F18	F20	F22	F24	F26
Wild-type													
1	W	W	W	W	W	W	W	W	W	W	W	W	W
2	W	W	W	W	W	W	W	W	W	W	W	W	W
3	W	W	W	W	W	W	W	W	W	W	W	W	W
4	W	W	W	W	W	W	W	W	W	W	W	W	W
mrt-1(e2661)													
1	W	W	W	M	M	F	VF	S					
2	W	W	W	W	W	M	M	M	F	S			
3	W	W	W	W	W	M	W	M	F	VF	S		
4	W	W	W	M	W	M	M	M	F	VF	S		
mrt-1(yp2)													
1	W	W	W	W	W	M	W	M	F	F	F	VF	S
2	W	W	W	W	W	W	W	W	M	M	M	F	VF
3	W	W	W	W	W	W	M	M	M	M	M	M	F
mrt-1(tm1354)													
1	W	W	W	W	W	M	W	M	F	S			
2	W	W	W	W	W	M	M	F	F	F	VF	S	
mrt-2(e2663)													
1	W	W	W	W	M	M	F	M	F	VF	VF	S	
2	W	W	M	M	M	M	M	M	F	VF	S		
3	W	W	M	W	M	M	F	F	VF	S			
4	W	W	M	F	S								
trt-1(ok410)													
1	W	W	W	W	M	M	M	M	F	F	VF	S	
2	W	W	W	W	W	W	M	F	VF	S			
3	W	W	W	W	W	W	W	M	M	F	F	VF	

W, wild-type, ~250 progeny per animal; M, medium, ~80 progeny per animal; F, few, ~20 progeny per animal; VF, very few, ~3–5 progeny per animal; S, sterile.
Mutants were backcrossed twice against wild-type to restore telomere length and two to four homozygous lines of the indicated genotype were followed by picking six L1s each line every two generations, as described previously (Ahmed and Hodgkin, 2000), for 26 generations. Brood size and sterility are indicated.

the SNM1 nuclease family. SNM1 proteins function in DNA repair and checkpoint responses to interstrand cross-links (ICLs), stalled replication forks and DSBs, as well as in telomere protection (Henriques and Moustacchi, 1980; Dronkert *et al*, 2000; Demuth *et al*, 2004; Jeggo and Lobrich, 2005; Freibaum and Counter, 2006; Lenain *et al*, 2006; van Overbeek and de Lange, 2006; Bae *et al*, 2008; Hazrati *et al*, 2008; Hemphill *et al*, 2008). Although previously described *C. elegans* DNA-damage response mutants that are deficient for telomerase activity *in vivo* are hypersensitive to DSBs and ICLs, *mrt-1* mutants are only deficient for ICL repair. Thus, MRT-1 defines a dual-domain ICL DNA-damage response protein that may process and interact with chromosome termini prior to telomerase-mediated telomere repeat addition.

Results

MRT-1 is required for telomerase activity in vivo

To identify non-essential mutations that compromise telomerase activity *in vivo* in *C. elegans*, genetic screens for ethylmethanesulphonate (EMS)-induced *mortal germline (mrt)* mutations that resulted in progressive telomere shortening and progressive sterility, accompanied by telomere–telomere fusions, were performed. Two alleles of *mrt-1*, *e2661* and *yp2*, were identified in such screens (Y Liu and S Ahmed, unpublished data) (Ahmed and Hodgkin, 2000). *mrt-1* mutants showed progressive reduction in progeny and eventual sterility comparable to *mrt-2* mutants and mutants defective for the *C. elegans* catalytic subunit of telomerase, *trt-1*, (Table I) accompanied by progressive telomere shortening over successive generations (Figure 1A and Figure 5). Although telomere length does fluctuate as N2 wild-type strains are propagated for multiple generations (Ahmed *et al*, 2001), wild-type telomeres appeared as diffuse bands on Southern blots, whereas telomeres of all *mrt-1* alleles appeared as discrete bands that shorten progressively (Figure 1A, right panel), as previously observed for *C. elegans* mutants that are deficient for telomerase mediated-telomere replication such as *trt-1*, *mrt-2*, *hus-1* and *hpr-17* (Ahmed and Hodgkin, 2000; Hofmann *et al*, 2002; Meier *et al*, 2006; Boerckel *et al*, 2007). In crosses between *mrt-1(e2661)* and wild-type, *mrt-1*$^{-/-}$ F2 siblings displayed telomere erosion accompanied by progressive sterility, whereas wild-type F2 siblings displayed neither phenotype, but did possess discrete telomeric restriction fragments inherited from the *mrt-1* background (Figure 1A, left panel, and data not shown). In addition, *mrt-1* strains displayed late-onset chromosome fusions, as indicated by reduced numbers of metaphase-arrested meiotic chromosomes in late-generation *mrt-1* mutants (Figure 1B and Supplementary Figure 1). The presence of end-to-end chromosome fusions was verified by isolation of X-autosome fusions from three independent *mrt-1* strains (Figure 1C). Genetic mapping of the dominant-chromosome-loss phenotype

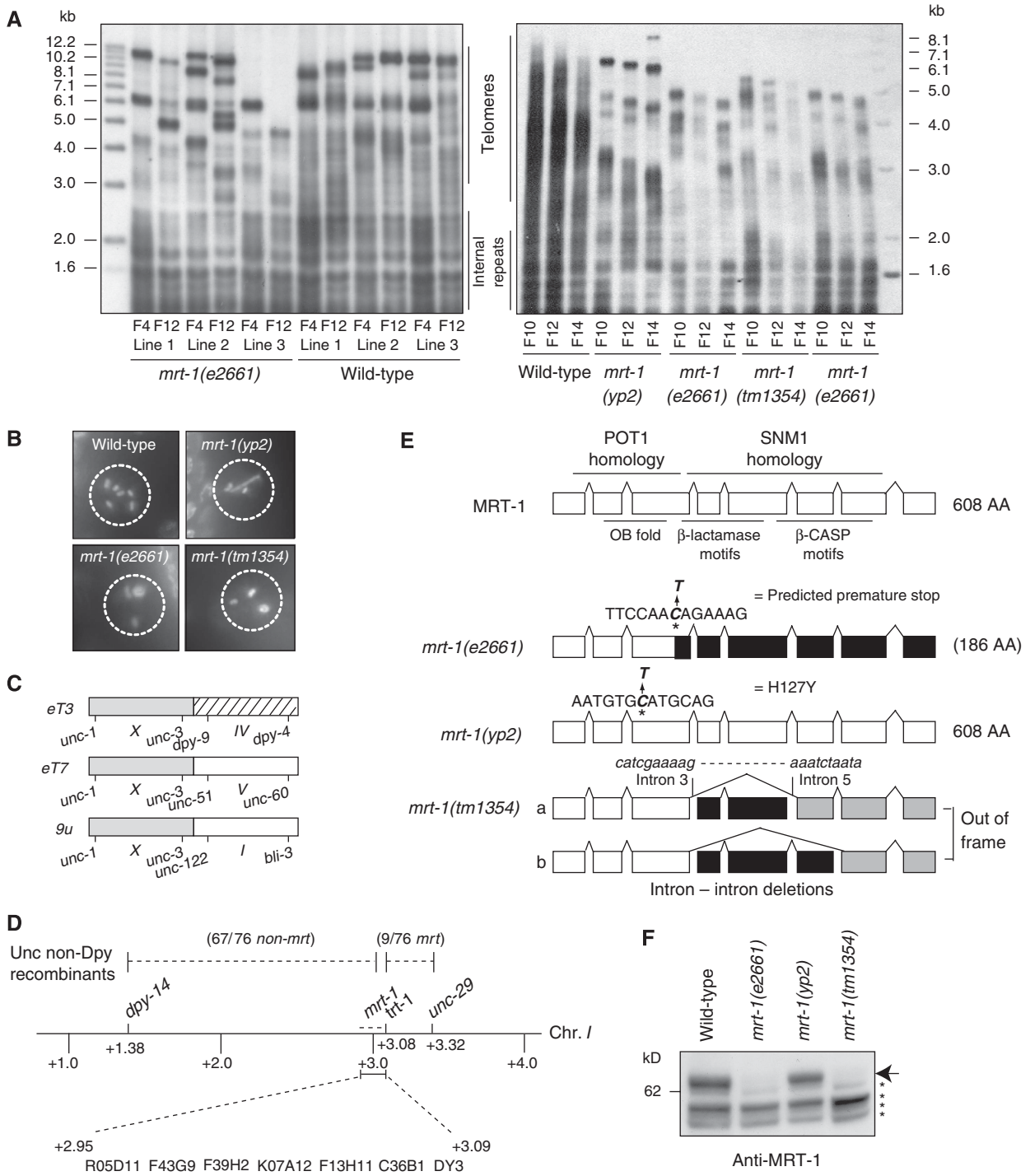

Figure 1 Characterization and genetic mapping of *mrt-1*. (**A**) *mrt-1* mutants display progressive telomere shortening. Southern blotting of genomic DNA with a telomere repeat-specific probe was performed as described previously (Ahmed and Hodgkin, 2000; Meier *et al*, 2006). F4 and F12 generations of three homozygous *mrt-1(e2661)* mutant and three homozygous wild-type siblings from a single outcross are shown in the left panel and three progressive generations of wild-type, *mrt-1(yp2)*, two lines of *mrt-1(e2661)* and *mrt-1(tm1354)* each are shown in the right panel. Internal-repeat signals (Wicky *et al*, 1996) and telomere signals are indicated. (**B**) DAPI staining of late-generation wild-type or mrt-1 worms. Representative oocyte nuclei, indicated by dashed circles, are shown. (**C**) X-autosome fusions, *eT3, eT7* and *9u*, isolated from independent *mrt-1(e2661)* strains. Visible markers used for mapping are indicated. (**D**) Map position of *mrt-1* as determined by three-factor crosses. The number of recombination events scored between *mrt-1* and *unc-29* is indicated in brackets. Cosmids covering the approximate genetic position of *mrt-1* are shown. (**E**) *mrt-1* gene structure and mutations. Point mutations are indicated in bold italics. Solid black boxes depict exons that are not translated due to the *e2661* premature stop codon or are missing as a consequence of altered *mrt-1* splicing in *tm1354*. In *tm1354*, the deletion within introns 3 and 5 leads to two alternatively spliced mRNAs indicated as (a) and (b) (see Supplementary Figure 2B), resulting in downstream exons to be out of frame (indicated in grey). (**F**) Western blot of protein extracts from wild-type and *mrt-1* mutant strains. The arrow indicates MRT-1 protein, asterisks indicate nonspecific bands.

Table II *mrt-1* complementation

Strain	Lines	Sterility
trt-1(ok410) unc-29/ ++	3	No*
trt-1(ok410) unc-29/trt-1(ok410) unc-29	6	Yes
mrt-1(e2661) dpy-5/ ++	4	No*
mrt-1(yp2) dpy-5/ ++	3	No*
++ trt-1(ok410) unc-29/dpy-5 mrt-1(e2661) ++	4	No*
++ trt-1(ok410) unc-29/dpy-5 mrt-1(yp2) ++	4	No*
+ trt-1(ok410) unc-29/mrt-1(tm1354) ++	3	No*
dpy-5 mrt-1(e2661)/ + mrt-1(tm1354)	4	Yes
dpy-5 mrt-1(yp2)/ + mrt-1(tm1354)	4	Yes

Trans-heterozygous analysis of *mrt-1* alleles with *trt-1*. *mrt-1* alleles were placed in *trans* to *trt-1* or to a different *mrt-1* allele (as shown) and progeny of several independent F1s were propagated as trans-heterozygotes (see Supplementary data) until sterility, while lines marked with an asterisk did not show any visible reduction in viability when propagated up to 15–20 generations.

of these independent fusions, which occurs when an X-autosome chromosome fusion is in *trans* to unfused chromosomes during meiosis, revealed tight genetic linkage of one end of the X chromosome with an end of an autosome in each case, confirming the formation of covalent end-to-end chromosome fusions (Figure 1C; see Supplementary data) (Ahmed and Hodgkin, 2000; Meier *et al*, 2006; Boerckel *et al*, 2007; Lowden *et al*, 2008). The former *mrt-1* phenotypes resemble *C. elegans* strains that are deficient in telomerase activity *in vivo* (Ahmed and Hodgkin, 2000; Hofmann *et al*, 2002; Meier *et al*, 2006; Boerckel *et al*, 2007).

Two- and three-factor crosses were used to map *mrt-1* to approximately +2.92 on Chromosome *I* (Figure 1D). Although *trt-1* is located nearby at +3.08, *mrt-1* mutations complemented *trt-1(ok410)* for progressive sterility when propagated as trans-heterozygotes, whereas failure to complement was observed between the *mrt-1* mutations *e2661* and *yp2*, indicating that these mutations correspond to a single gene that is distinct from *trt-1* (Table II; and data not shown). Failure to complement *trt-1(ok410)* was previously reported for three independent alleles of *trt-1 (e2727*, *yp1* and *tm899*), thereby clearly defining the *C. elegans* telomerase reverse transcriptase (Meier *et al*, 2006). BLAST searches of predicted proteins to the left of *trt-1* revealed an open reading frame, F39H2.5, encoding a protein with an N-terminal domain homologous to the second OB-fold of POT1 telomere-binding proteins and a C-terminal domain containing the metallo-β-lactamase and β-CASP motifs characteristic of the SNM1 family of nucleic acid processing factors (Figures 1E and 2, see below). Isolation and sequencing of the *mrt-1* cDNA confirmed the predicted 608-amino-acid POT1 OB-fold/SNM1 dual-domain protein (Figure 1E and Supplementary Figure 2). Sequencing of F39H2.5 from wild-type, *mrt-1(e2661)* and *mrt-1(yp2)* revealed independent C-to-T transition mutations in *e2661* and *yp2*, predicted to create stop codon and missense mutations, respectively (Figure 1E). The *mrt-1(yp2)* missense mutation results in an H127Y amino-acid change, thus altering an amino acid whose charge is conserved in the OB2-fold of most POT1 proteins (Figure 2A).

Upon identification of the *mrt-1* gene based on our forward genetic experiments, a deletion of this locus, *tm1354*, was kindly generated by Shohei Mitani. The *tm1354* deletion eliminates several exons of the C-terminal SNM1 nuclease domain, including conserved amino-acid motifs that are relevant for ICL repair in yeast Pso2p (Niegemann and Brendel, 1994; Li and Moses, 2003 and Figure 1E). RT–PCR of *mrt-1* cDNA from *tm1354* animals revealed two mRNAs predicted to result in truncated, out-of-frame proteins (Figure 1E and Supplementary Figure 2B). The *tm1354* deletion was isolated under conditions that generate many additional lesions in a strain's genome (Gengyo-Ando and Mitani, 2000). Therefore, two- and three-factor crosses were performed to show that a locus tightly linked to the *tm1354* deletion conferred progressive telomere erosion phenotypes characteristic of *C. elegans* telomerase mutants (Figure 1A and B and Table I, and data not shown). Further, the *tm1354* deletion failed to complement the *mrt-1* alleles *e2661* and *yp2* for progressive sterility and late-onset end-to-end chromosome fusion phenotypes, but complemented *trt-1(ok410)* (Table II). Although a strain containing the *tm1354* deletion was previously mentioned to display progressive telomere shortening (Raices *et al*, 2008), the identification of independent alleles of this locus, as well as the genetic mapping and complementation tests described here, indicate that the telomere shortening observed in the *tm1354* strain is caused by a defect in the *mrt-1*/F39H2.5 gene.

A polyclonal antibody raised against full-length MRT-1 detected equivalent levels of full-length MRT-1 and MRT-1(H127Y) in wild-type and *mrt-1(yp2)* worm extracts, respectively (Figure 1F). Thus, the POT1-related OB2 domain of MRT-1 is required for telomerase activity *in vivo*. In contrast, no MRT-1 protein was detected in the *e2661* nonsense mutation and *tm1354* deletion extracts (Figure 1F and data not shown), indicating that these mutations are likely to be null alleles of *mrt-1*/F39H2.5, a non-essential gene required for *de novo* telomere repeat addition in *C. elegans*.

mrt-1 encodes a dual-domain protein

The N-terminal domain of *C. elegans* MRT-1 shares sequence homology with the second OB-fold of POT1 proteins (Figure 2A and Supplementary Figure 3). Single-stranded telomeric DNA-binding proteins commonly contain two adjacent N-terminal OB-folds, OB1 and OB2 (Horvath *et al*, 1998; Lei *et al*, 2003, 2004; Theobald and Wuttke, 2004). In addition to MRT-1, the *C. elegans* genome encodes two short proteins with homology to the second OB2-fold of POT1, F57C2.3 (CeOB1) and 3R5.1 (Figure 2A and Callebaut *et al*, 2002; Raices *et al*, 2008). The OB2-folds of MRT-1, F57C2.3 (CeOB1) and 3R5.1 are closely related and likely evolved from a single ancestral OB2-fold gene. A fourth *C. elegans* gene, B0280.10 (CeOB2), is homologous to the first OB-fold of POT1, OB1 (Figure 2A and Raices *et al*, 2008). The tandem OB-fold structure typical of POT1 proteins has been subjected to fission and duplication in *C. elegans*. Thus, we originally identified *mrt-1*/F39H2.5 based on the genetic map position of the *mrt-1(e2661)* telomerase-deficient mutant, and three additional *C. elegans* genes were identified based on their homology to POT1: B0280.10, F57C2.3 and 3R5.1. While this study was in progress, these genes were independently identified as POT1 homologues (Raices *et al*, 2008). We designate the *C. elegans* gene name for these genes as '*pot*', for 'homologous to Protection of Telomeres 1(Pot1)', where *pot-1* is B0280.10 (CeOB2) *pot-2* is F57C2.3 (CeOB1) and *pot-3* is 3R5.1 (Figure 2A) (Raices *et al*, 2008; Lowden *et al*, 2008). These genes display sequence similarity to, and evolved from, POT1,

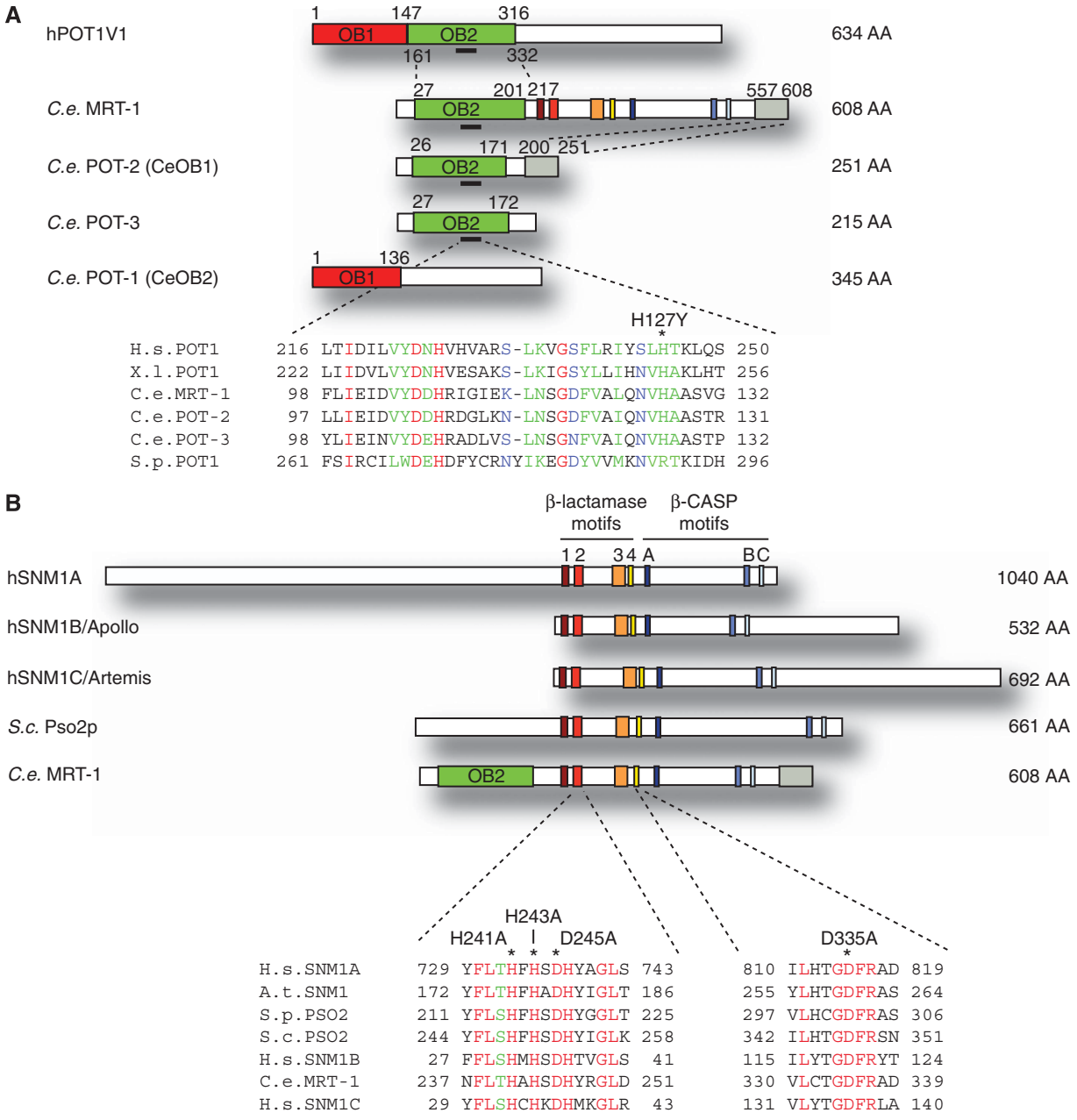

Figure 2 MRT-1 shares sequence homology with POT1 and SNM1 proteins. (**A**) Protein domain structure of hPOT1, MRT-1 and the three additional *C. elegans* OB-fold domain proteins with homology to POT1. The conserved histidine H127Y (asterisk) mutated in the MRT-1 protein of *mrt-1(yp2)* is indicated. The region of homology around H127Y of the three *C. elegans* (*C.e.*) OB2-fold proteins aligned with the respective POT1 domains of *Homo sapiens* (*H.s.*), *Xenopus laevis (X.l)* and *Saccharomyces pombe (S.p.)* is shown. No clear alignment could be obtained for *Arabidopsis thaliana* POT1 within this region. Sequence alignments were generated using Pole BioInformatique Lyonnais ClustalW (http://pbil.ibcp.fr/htm/index.php). Red shading reflects sequence identity, green strong and blue weak similarity. (**B**) Protein domain structure of *C.e.* MRT-1, *S. cerevisiae (S.c.)* Pso2p and human SNM1A, SNM1B/Apollo and SNM1C/Artemis. A multiple sequence alignment of the HxHxDH and β-CASP motif-4 nuclease domains is shown below. Amino acids depicted on top of the alignment indicate amino-acid changes introduced into MRT-1 to generate MRT-1(4mut) (see Figure 3 and Supplementary data).

and their functions may reflect (1) one or more functions of ancestral POT1, including but not limited to 'protection of telomeres', or (2) derived functions that may be unrelated to the ancestral protein. Since F39H2.5/*mrt-1* contains homology to two conserved proteins, POT1 and SNM1, the gene name *mrt-1* is used, based on the Mortal Germline phenotype of *mrt-1* mutants (Ahmed and Hodgkin, 2000). MRT-1 is the only *C. elegans* POT1-like OB-fold protein that is required for telomerase activity *in vivo* (Figure 1), whereas the *pot-1*(CeOB2) and *pot-2*(CeOB1) genes may repress telomerase activity or recombination at telomeres (Raices *et al*, 2008; M Lowden and S Ahmed, unpublished data).

The C-terminus of MRT-1 corresponds to the sole *C. elegans* homologue of SNM1 proteins (Figure 1E and Figure 2B), which are members of the nucleolytic DNA- and RNA-processing β-CASP (metallo-β-lactamase-associated CPSF-Artemis-SNM1/PSO2) protein family (Aravind, 1999; Callebaut *et al*, 2002; Dominski, 2007). *Saccharomyces*

cerevisiae Pso2p, and mammalian SNM1A and SNM1B/Apollo promote ICL repair (Henriques and Moustacchi, 1980; Demuth *et al*, 2004; Bae *et al*, 2008; Hazrati *et al*, 2008; Hemphill *et al*, 2008). In addition, SNM1B/Apollo and SNM1C/Artemis contribute to telomere end protection (Rooney *et al*, 2003; Freibaum and Counter, 2006; Lenain *et al*, 2006; van Overbeek and de Lange, 2006).

The OB-fold/SNM1 dual-domain structure of MRT-1 is observed for the closely related *Caenorhabditis* species *remanei* and *briggsae*, but was not predicted from genome sequences of the distantly related parasitic nematodes *Brugia malayi* and *Trichinella spiralis* (data not shown). Thus, fusion of POT1 OB2 and SNM1 domains to create the *mrt-1* gene may have occurred within the Nematode phylum.

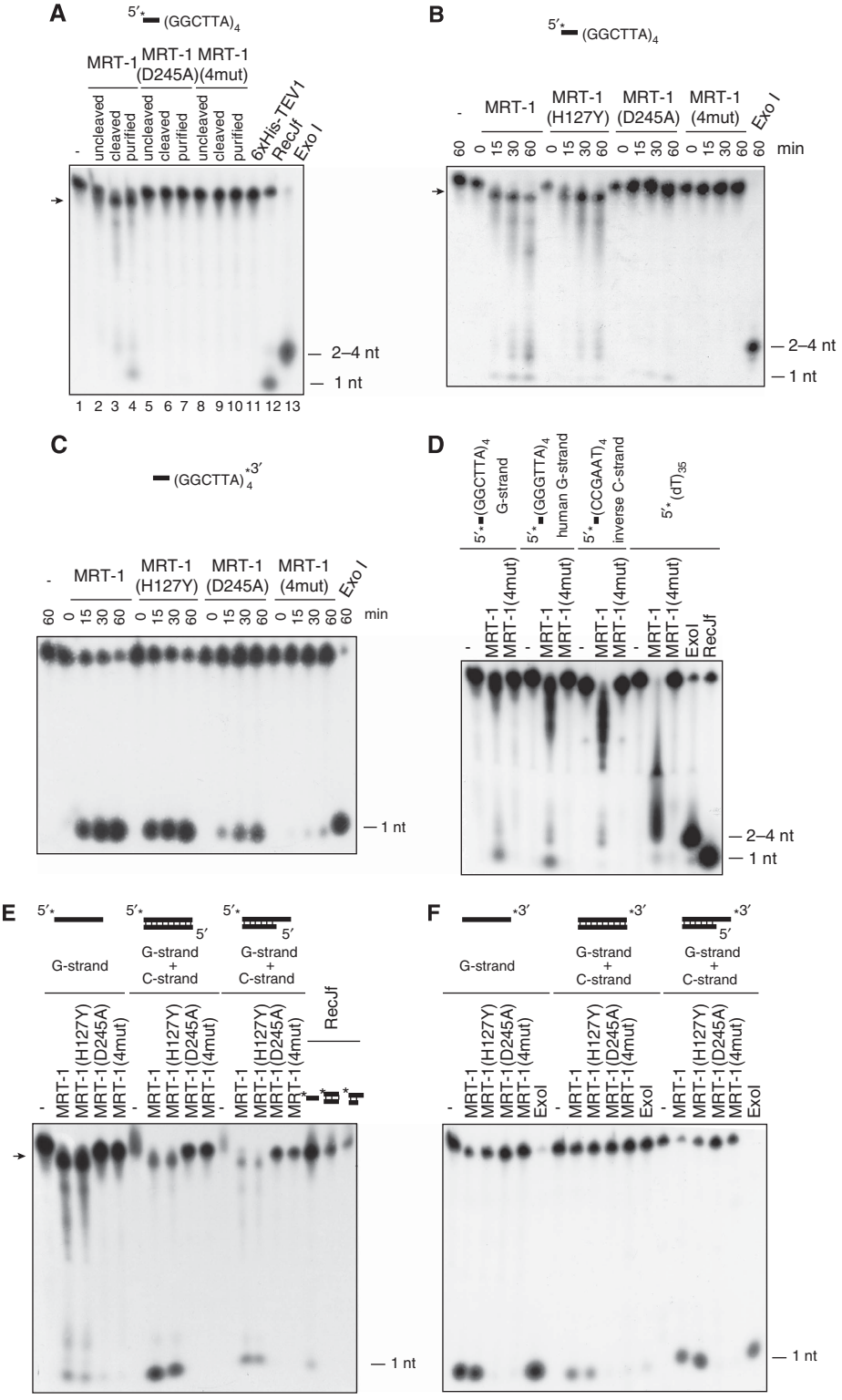

MRT-1 acts as a nuclease in vitro

To determine whether MRT-1 harbours nucleolytic activity as implied by its sequence homology to SNM1 proteins, we purified wild-type, the MRT-1(H127Y) OB-fold mutant, and two putative nuclease-dead mutant versions of MRT-1, MRT-1(D245A) and MRT-1(4mut), from *Escherichia coli* (Supplementary Figure 4A). The MRT-1(D245A) protein contains an aspartate to alanine mutation in the conserved HxHxDH signature motif, which comprises residues predicted to participate in zinc coordination (histidines) and hydrolysis (aspartate) at the active site (Figure 2B and Carfi *et al*, 1995). In budding yeast, this mutation diminishes the *in vitro* 5′-to-3′ nuclease activity of Pso2p and leads to an ICL-repair defect *in vivo* (Li *et al*, 2005). The corresponding mutation abolishes the *in vitro* 5′ exonuclease activity of mammalian SNM1A (Hejna *et al*, 2007) and reduces the endonucleolytic activity of SNM1C/Artemis that is observed in the presence of DNA-PK (Pannicke *et al*, 2004). However, as this single amino-acid change does not abolish SNM1 nuclease activity in all cases (Pannicke *et al*, 2004), we also disrupted the putative catalytic core of MRT-1 with four mutations (4mut): a HxHxDH-to-AxAxAH triple mutation and a D335A substitution in motif-4 (Figure 2B and Poinsignon *et al*, 2004). Wild-type and mutant versions of recombinant MBP-6 × His–TEV–MRT-1 were purified over a TALON column resulting in a ~120-kDa MBP-6 × His–TEV–MRT-1 band (Supplementary Figure 4A). Cleavage with TEV protease followed by a second purification step yielded untagged full-length MRT-1 (Supplementary Figure 4A and Supplementary data). Cleaved and purified MRT-1 protein exhibited 3′ nuclease activity as revealed by complete removal of one or more 3′ nucleotides from a 5′-end-labelled substrate (Figure 3A, arrow, and Figure 3B, arrow), accompanied by a smear of additional degradation products, which includes minor stalling points and release of the terminal 5′ nucleotide. This activity was not observed for TEV protease alone (Figure 3A, lane 11). Importantly, no nuclease activity was observed with MRT-1(D245A) or MRT-1(4mut) mutants, indicating that this activity requires conserved residues in the MRT-1 nuclease domain (Figure 3A, lanes 5–10; Figure 3B). A time-course experiment using MRT-1 and MRT-1 (H127Y), which contains the POT1 OB-fold substitution that abolishes telomerase activity *in vivo*, indicated that the nuclease activity of MRT-1, apparent by the complete removal of one or more 3′ nucleotides (arrow), as well as a smear of degradation products, is not affected by the OB-fold mutation (Figure 3B). Removal of the N-terminal epitope tags from MRT-1 promoted degradation of 5′-end-labelled substrates, accompanied by release of a small amount of 5′ mononucleotide, which might correspond to either a weak 5′ nuclease activity or a processive 3′ nuclease activity that completely degrades the oligonucleotide substrate (Figure 3A and B). To distinguish between these possibilities, MRT-1 was incubated with a 3′-end-labelled substrate. A single 3′ mononucleotide was released from 3′-end-labelled substrate in Figure 3C, in a nuclease domain-dependent manner. Thus, MRT-1 functions as a 3′–5′ nuclease, similar to the 3′–5′ exonuclease *Exo*I control (Figure 3C). If MRT-1 were a processive 5′-to-3′ nuclease, then a ladder of products would have been observed for the 3′-end-labelled substrate in Figure 3C. Consistently, incubation of various dilutions of MRT-1 protein with 3′-end-labelled G-strand substrate failed to reveal any cleavage intermediates expected for 5′-to-3′ exonuclease activity (Supplementary Figure 4E). We considered the possibility that the 5′ phosphate of 5′-end-labelled substrates might elicit 5′-to-3′ nuclease activity by MRT-1, as has been observed for SNM1 (Hejna *et al*, 2007), but addition of a cold 5′ phosphate to 3′-end-labelled ssDNA substrate did not promote the formation of an n-1 product by MRT-1, and resulted exclusively in release of the terminal 3′ nucleotide (data not shown). While MRT-1 and MRT-1(H127Y) showed comparable efficiency in cleaving the terminal 3′-labelled substrate, MRT-1(D245A) and MRT-1(4mut) exhibited strongly reduced kinetics and absence of activity, respectively (Figure 3C). Thus, our results indicate that MRT-1 functions as a 3′-to-5′ nuclease *in vitro*.

Use of n-1, n-2 and n-3 *C. elegans* G-strand oligonucleotide size markers revealed that an n-3 molecule is the major product of the MRT-1 nuclease for the 5′-end-labelled *C. elegans* G-strand substrate (Supplementary Figure 4C). Dilutions of MRT-1 protein revealed a smear of n-1, n-2 and n-3 degradation products, which occur during the rapid generation of the n-3 product (Supplementary Figure 4D). Thus, MRT-1 does not act as an endonuclease that chops off three 3′ nucleotides at the 3′ end of the *C. elegans* G-strand substrate, but rather as a processive 3′-to-5′ exonuclease that stalls at the n-3 position. Various 5′-end-labelled substrates, including telomeric G-strand and C-strand oligonucleotides and $(dT)_{35}$, were efficiently processed by MRT-1, although different patterns of nucleolytic activity were observed (Figure 3D). The oligo(dT) substrate was more severely degraded, suggesting that the activity of MRT-1 may depend on the sequence or structure of its substrates. In an attempt to address the various nucleolytic patterns of MRT-1 on different oligonucleotides (Figure 3D), we examined the effect of

Figure 3 MRT-1 acts as a 3′ nuclease *in vitro*. (**A**) 70 nM of MRT-1, MRT-1(D245A) and MRT-1(4mut) from different purification steps were incubated with 5 nM of a *C. elegans* telomeric G-strand oligonucleotide labelled at the 5′ end (asterisk). The line before the oligonucleotide sequence shown depicts an invariant linker sequence (see Supplementary data). 6 × His–TEV1 extracts were tested for contaminating nuclease activity (lane 11). The 5′-to-3′ nuclease RecJf and the 3′-to-5′ nuclease *Exo*I were used as controls (lanes 12 and 13, respectively). 1-nt products generated by RecJf and 2- to 4-nt products generated by *Exo*I are indicated. The arrow indicates the reduced size oligonucleotide band due to nuclease activity. For panel A, lane 2, it is difficult to assess the degree of nucleolytic activity for uncleaved MRT-1 due to a gel-running artefact. (**B**) Time-course experiment of MRT-1, MRT-1(H127Y), MRT-1(D245A) and MRT-1(4mut) nuclease activity on a 5′ labelled (asterisk) *C. elegans* telomeric G-strand oligonucleotide. 70 nM of protein were incubated with 5 nM of 5′ labelled oligonucleotide and aliquots were taken at the time points indicated. 2- to 4-nt products generated by *Exo*I and 1-nt products are indicated. The line drawn before the oligonucleotide sequence depicts an invariant linker sequence (see Supplementary data). The arrow indicates the reduced size band due to nuclease activity. (**C**) Time-course of MRT-1, MRT-1(H127Y), MRT-1(D245A) and MRT-1(4mut) nuclease activity on a 3′ labelled (asterisk) *C. elegans* telomeric G-strand oligonucleotide performed as described in panel B. (**D**) 70 nM MRT-1 and MRT-1(4mut) were incubated with 5 nM of various 5′ labelled single-stranded oligonucleotides for 1 h. (**E**) 70 nM MRT-1 and MRT-1(4mut) proteins were incubated with 1 nM of single- or double-stranded 5′ labelled DNA substrates as indicated (see Supplementary data). 1-nt products as generated by RecJf are indicated. The arrow indicates the reduced size band due to nuclease activity. (**F**) MRT-1 and MRT-1(4mut) proteins were incubated with single- or double-stranded 3′ labelled (asterisk) DNA substrates as described in panel E. 1-nt products as generated by *Exo*I are indicated.

MRT-1 on n-1, n-2 and n-3 *C. elegans* G-strand substrate molecules, where the major product of the full-length G-strand substrate is an n-3 molecule. The n-1 or n-2 substrates were rapidly cleaved to yield an n-3 product, whereas the n-3 substrate was resistant to the strong 3′-to-5′ exonuclease activity of MRT-1, which rapidly removes 3′ nucleotides from full-length, n-1 and n-2 G-strand substrate molecules (Supplementary Figure 4F). Note that MRT-1 created a weak smear of degradation products for all single-stranded G-strand oligonucleotides, including the n-3 substrate. A major n-3-mer product was also generated when MRT-1 was incubated with double-stranded *C. elegans* G-strand substrate, where the G-strand was 5′-end-labelled (Figure 3E and data not shown). Thus, when three nucleotides are removed

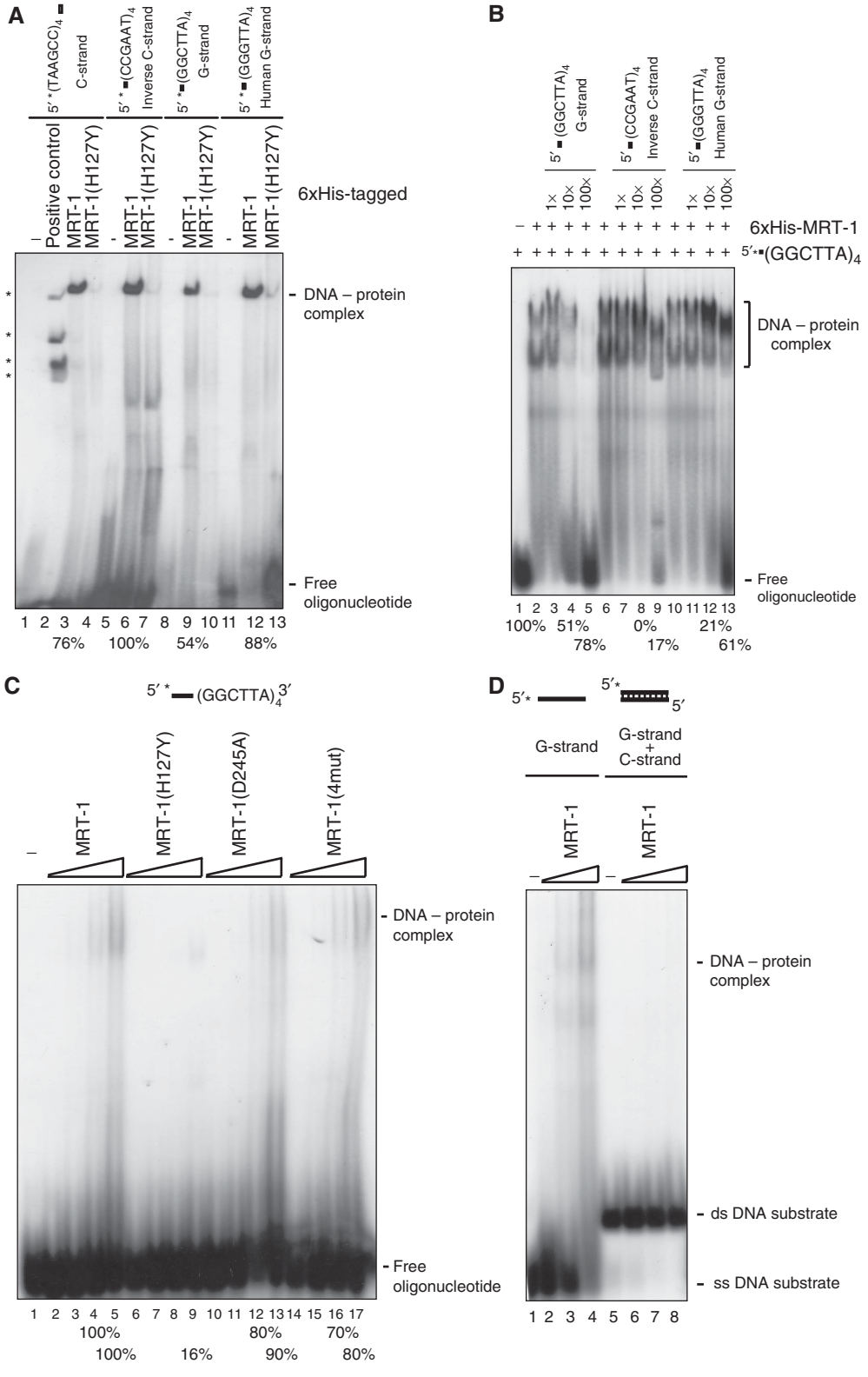

from the *C. elegans* G-strand substrate terminating in GGCTTA to yield an n-3 molecule terminating in TTAGGC, the processive 3′-to-5′ nuclease activity of MRT-1 is inhibited. Raising the incubation temperature of the MRT-1 cleavage reaction from 20 to 37°C resulted in uniform laddering of a *C. elegans* telomeric G-strand substrate (Supplementary Figure 4B), analogous to the oligo(dT) substrate at 20°C. This temperature-sensitive effect may reflect altered structure of the 3′ end of the n-3-mer, or perhaps increased processivity of MRT-1 protein, at 37°C. Formal proof that MRT-1 harbours a 3′-to-5′ exonuclease activity that may possess a degree of structure or sequence specificity awaits detailed characterization of various substrate molecules and how they are processed by MRT-1.

Analysis of the activity of MRT-1 on 5′-end-labelled, blunt, double-stranded DNA substrates or on a substrate with a 3′ telomeric overhang resulted in release of both 3′ and 5′ nucleotides (Figure 3E). To test whether release of the 5′ nucleotide from either substrate was due to 5′–3′ nuclease activity, analogous 3′-end-labelled substrates were examined, but only the 3′ nucleotide was released, and no n-1 band or additional banding pattern was observed (Figure 3F). n-1, n-2 and n-3 size markers indicated that an n-1 product could have been detected for 3′-end-labelled substrates if it occurred as a consequence of a non-processive 5′ nuclease activity (Supplementary Figure 4C, D and F). Thus, the relatively strong release of the 5′ terminal nucleotide from 5′-end-labelled dsDNA substrates occurs as a consequence of the 3′-to-5′ polarity of the MRT-1 nuclease.

We conclude that MRT-1 is a processive 3′-to-5′ exonuclease, which can degrade single-stranded substrates, which can be repressed by specific substrate configurations, and which can act to release the terminal 5′ nucleotides of substrates that are degraded with 3′-to-5′ polarity. The nuclease activity of MRT-1 is dependent on its SNM1 nuclease domain, but this activity is not affected by the H127Y POT1 OB-fold mutation. Note that the nuclease activities displayed by MRT-1 *in vitro* may be affected by protein modification or protein–protein interactions, and could be substrate dependent. The strong activity of MRT-1 on non-telomeric substrates is significant and not unexpected, as MRT-1 is not telomere-specific but also functions a general ICL-repair protein (see Figure 6, below).

MRT-1 binds single-stranded DNA in vitro

Although two adjacent N-terminal OB-folds in human POT1 are required for POT1 to bind single-stranded telomeric DNA *in vitro* (Lei *et al*, 2004), the sequence homology of MRT-1 is restricted to the second OB-fold of POT1 (Figure 2A). Electrophoretic mobility-shift assays revealed that 6 × His–MRT-1 bound to a radiolabelled single-stranded $(GGCTTA)_4$ *C. elegans* telomeric G-strand oligonucleotide (Figure 4A, lane 9). Furthermore, MRT-1 bound to various single-stranded oligonucleotides, including a *C. elegans* C-strand, an inverse C-strand and a human G-strand, with comparable affinity (Figure 4A, lanes 3, 6 and 12). DNA competition experiments revealed that an unlabelled *C. elegans* telomeric G-strand oligonucleotide was consistently able to compete with an MRT-1 complex bound to a radiolabelled G-strand oligonucleotide with at least 10-fold greater affinity than an unlabelled *C. elegans* telomeric C-strand oligonucleotide (Figure 4B and Supplementary Figure 5A). For reasons that are unclear, epitope-tagged MRT-1 band shifts were resolved as either single or double bands in different experiments, even when MRT-1 protein from the same protein purification was used (Figure 4B and Supplementary Figure 5A).

The *mrt-1(yp2)* allele deficient for telomerase activity *in vivo* encodes an H127Y protein mutation that affects a conserved charged residue in its OB-fold (Figures 1E and 2A) and thus may affect DNA binding. In comparison to 6 × His–MRT-1, an equivalent concentration of 6 × His–MRT-1(H127Y) had strongly diminished affinity for all single-stranded oligonucleotides tested, including *C. elegans* G-strand telomere repeats (Figure 4A, lanes 4, 7, 10 and 13). To assess the DNA-binding activity of untagged MRT-1, MBP-6 × His–TEV–MRT-1 fusion proteins were purified and cleaved with TEV protease. Similar to 6 × His-tagged MRT-1, binding of TEV-cleaved MRT-1(H127Y) to a G-strand oligonucleotide was reduced five- to eight-fold in comparison with wild-type MRT-1 (Figure 4C). Untagged MRT-1 protein does not show the crisp band shifts observed for epitope-tagged MRT-1 (Figure 4 and Supplementary Figure 5). We hypothesized that the smeary band shifts might occur as a consequence of the nuclease activity of MRT-1, but they remained smeary for nuclease-dead versions of MRT-1, which bound *C. elegans* G-strand substrate with an affinity similar as MRT-1 (Figure 4C). Smeary band shifts were consistently observed

Figure 4 MRT-1 binds single-stranded DNA *in vitro*. (**A**) Gel-shift analysis of 200 nM purified 6 × His–MRT-1 or 6 × His–MRT-1(H127Y) with 5 nM of the indicated oligonucleotide substrates (top; also listed in Supplementary data) in the presence of poly(dI–dC). The position of radioactive labels is indicated by asterisks and the invariant linker sequence of each oligonucleotide is indicated as described for Figure 3. DNA-binding activities of a bacterial *in vitro* translation extract were used as a DNA-binding control (see lane 2, 'positive control'). DNA–protein complexes and free oligonucleotides are indicated. Percentages shown on the bottom of the gel indicate relative intensities of the shifted DNA–protein complexes (the shift of lane 6 being set to 100%). (**B**) Competition experiments of 6 × His–MRT-1 bound to a 5′ labelled (asterisk) single-stranded G-strand oligonucleotide followed by addition of increasing amounts of the indicated unlabelled oligonucleotides. Note that an inverse C-strand oligonucleotide is used for competition with the labelled G-strand oligonucleotide to avoid formation of double-stranded DNA. In this experiment, MRT-1 protein shifts as two different complexes with the radiolabelled oligonucleotide, which are equally competed by addition of unlabelled competitor oligonucleotides. Percentages shown on the bottom indicate relative amounts of free radiolabelled oligonucleotide with the unbound oligonucleotide (lane 1) set to 100%. (**C**) Gel-shift analysis of TEV-cleaved and dialysed MRT-1 wild-type and mutant proteins. Wild-type and mutant proteins were incubated with 5 nM 5′ labelled single-stranded G-strand oligonucleotide using increasing protein concentrations of 17 nM, 50 nM, 150 nM, 450 nM in the presence of poly(dI–dC) as described in panel A. (**D**) Gel-shift analysis of TEV-cleaved and dialysed MRT-1 wild-type with single-stranded and double-stranded substrates. TEV-cleaved and dialysed wild-type MRT-1 protein (50, 150 and 450 nM) was incubated with 5 nM 5′ labelled single-stranded or double-stranded DNA substrates (see Supplementary data) in the presence of poly(dI–dC). Single-stranded and double-stranded DNA and protein–DNA complexes are indicated on the right. Note that single-stranded and double-stranded DNA run differently in native gels. Relative intensities of DNA–protein complexes were measured between lanes for single-stranded and double-stranded DNA containing identical protein concentrations after subtraction of the background signal. The intensities of the DNA–protein complexes formed with double-stranded DNA were 9 and 7% of that formed with single-stranded DNA for 150 and 450 nM MRT-1 (lane 7 compared to lane 3 and lane 8 compared to 4), respectively.

using several different protein purification protocols to purify MRT-1, and for many electrophoresis conditions, suggesting that non-static DNA–protein interactions may be an inherent biophysical property of MRT-1. The positively charged 6 × His-tag may non-specifically stabilize the interaction of MRT-1 with DNA (Figure 4A and B). Using concentrated untagged MRT-1 we found that 1.8 μM MRT-1 was required to fully shift the oligonucleotide substrate, whereas 600 nM MRT-1 shifted approximately 50% of the substrate (Supplementary Figure 5B). MRT-1 binding to double-stranded DNA substrates generated by annealing telomeric G-strand and C-strand oligonucleotides was reduced at least 10-fold in comparison with binding to single-stranded DNA (Figure 4D, and data not shown). Thus, MRT-1 can interact with various DNA substrates *in vitro*, and this biochemical property may be biologically meaningful as it is disrupted by an OB-fold mutation that abolishes telomerase activity *in vivo*.

Efforts to determine MRT-1 localization *in vivo* by indirect immunofluorescence using an anti-MRT-1 antibody (Figure 1F) were unsuccessful (B Meier, T Lee, S Ahmed, A Gartner, unpublished data), consistent with other reports that have failed to detect endogenous mammalian SNM1 proteins by immunofluorescence (Dronkert *et al*, 2000; Lenain *et al*, 2006; van Overbeek and de Lange, 2006). Further, the MRT-1 antibody was not effective for chromatin immunoprecipitation of telomeric DNA (J Hall and S Ahmed, unpublished data). Introduction of the wild-type *mrt-1(+)* genomic DNA locus or MRT-1::GFP constructs in the *mrt-1 (tm1354)* mutant backgrounds using either complex extrachromosomal arrays or microparticle bombardment resulted in undetectable or low expression of MRT-1 protein as assessed by western blotting and failed to rescue the *mrt-1* mutant ICL hypersensitivity phenotype (B Meier, L Barber, S Boulton, S Ahmed, A Gartner, unpublished data).

MRT-1 acts in the same pathway as MRT-2 and TRT-1 for telomere replication

To determine whether *mrt-1*, telomerase and *mrt-2* act in the same genetic pathway of telomere elongation, *mrt-1 trt-1* and *mrt-1; mrt-2* double mutants were generated for comparison with the respective single mutants. Mutants were grown to sterility, which occurred at approximately the same generation (data not shown), and the rate of telomere shortening was analysed by Southern blotting (Figure 5A and B). The rates of telomere shortening in *mrt-1(yp2) trt-1* or *mrt-1(e2661); mrt-2* double mutants, 106 ± 42 and 128 ± 30 bp per generation, respectively, were not significantly different from those of the single mutants, *mrt-1(yp2)* (106 ± 35 bp); *mrt-1(e2661)* (114 ± 26 bp); *trt-1* (125 ± 22 bp) and *mrt-2* (129 ± 30 bp) (Figure 5C). Therefore, these three genes appear to act in a single pathway to facilitate telomere repeat addition by telomerase *in vivo*.

MRT-1 defines an ICL-damage response pathway

Subunits of the 9-1-1 DNA-damage response complex and its RFC clamp loader *hpr-17* orchestrate DNA-damage signalling and repair of ionizing radiation (IR)-induced DSBs. Additionally, they are required for telomerase-mediated telomere length maintenance (Ahmed and Hodgkin, 2000; Hofmann *et al*, 2002; Boerckel *et al*, 2007). This dual function, coupled with observations that many additional proteins that interact with DSBs also function at normal telomeres (d'Adda di Fagagna *et al*, 2004), suggested that the DSB-repair function of the 9-1-1 complex may be relevant to telomerase-dependent telomere replication. Given that *mrt-1* and *mrt-2* act in a single telomere replication pathway (Figure 5A and C), we asked whether *mrt-1* shares the DSB-repair functions of the 9-1-1 complex by testing their sensitivity to ionizing radiation. DNA DSBs in germ cells are predominately repaired by homologous recombination in a manner that is dependent on the 9-1-1 DNA-damage response complex (Clejan *et al*, 2006). Quantification of the survival rates of progeny derived from γ-irradiated L4 larvae revealed that *mrt-2* was hypersensitive to IR-induced DSBs (Ahmed and Hodgkin, 2000), whereas *mrt-1* displayed a dose–response survival curve that was not significantly different from that of the wild-type (Figure 6A).

The mammalian SNM1C/Artemis protein is known to facilitate telomere capping and plays a role in non-homologous end-joining (NHEJ)-mediated DSB repair (Richie *et al*, 2002; Rooney *et al*, 2003). Since MRT-1 is the only *C. elegans* protein bearing sequence homology to the SNM1 family, we examined whether it too plays a role in NHEJ. In contrast to strains deficient for any of the core NHEJ subunits *lig-4*, *cku-70* or *cku-80* (Clejan *et al*, 2006), *mrt-1* mutant strains did not display defects in an assay for NHEJ-mediated DSB repair (Supplementary Figure 6). Thus, *mrt-1* is not required for NHEJ- or homologous recombination-mediated DSB repair.

As we did not observe a role for MRT-1 in either DSB repair or NHEJ, we considered whether it may instead be required for ICL repair, analogous to yeast Pso2p and human SNM1A (Hazrati *et al*, 2008). We tested *mrt-1(yp2)* and *mrt-1(e2661)* for their sensitivity to DNA ICLs and found that both mutant alleles displayed hypersensitivity to trimethylpsoralen photoactivated by UVA radiation (UV-TMP) compared with wild-type (Figure 6B). Given the specific defect of MRT-1 in DNA cross-link repair, we also tested the previously identified telomerase-deficient 9-1-1 DNA-damage response complex mutants *mrt-2* and *hus-1*, both of which were even more sensitive to UV-TMP than *mrt-1* (Figure 6B). Interestingly, *mrt-1(e2661); mrt-2(e2663)* and *mrt-1(yp2); mrt-2(e2663)* double mutants were not more sensitive than *mrt-2* single mutants (Figure 6C and D), indicating that *mrt-1* and the 9-1-1 complex may function in a common pathway to promote ICL repair.

Discussion

We have identified MRT-1 as a new factor required for telomerase-mediated telomere repeat addition *in vivo* using unbiased genetic screening and positional cloning. MRT-1 is a dual-domain protein comprised of an N-terminal region with a POT1-like OB2-fold domain and a C-terminus homologous to the Pso2/SNM1 family of nucleases.

Four POT1-related OB-fold proteins exist in *C. elegans*, yet MRT-1 is the only POT-1 OB-fold protein that is essential for telomere-repeat addition by telomerase. POT1 duplications have occurred several times during evolution and, once duplicated, POT1-like proteins tend to evolve rapidly and adopt distinct telomere-related functions. Mutation of one of three *Arabidopsis* POT1 genes abrogates telomerase activity *in vivo* and *in vitro* (Shakirov *et al*, 2005; Surovtseva *et al*, 2007). The former results mirror evidence from organisms that contain a single essential POT1-related gene (Baumann

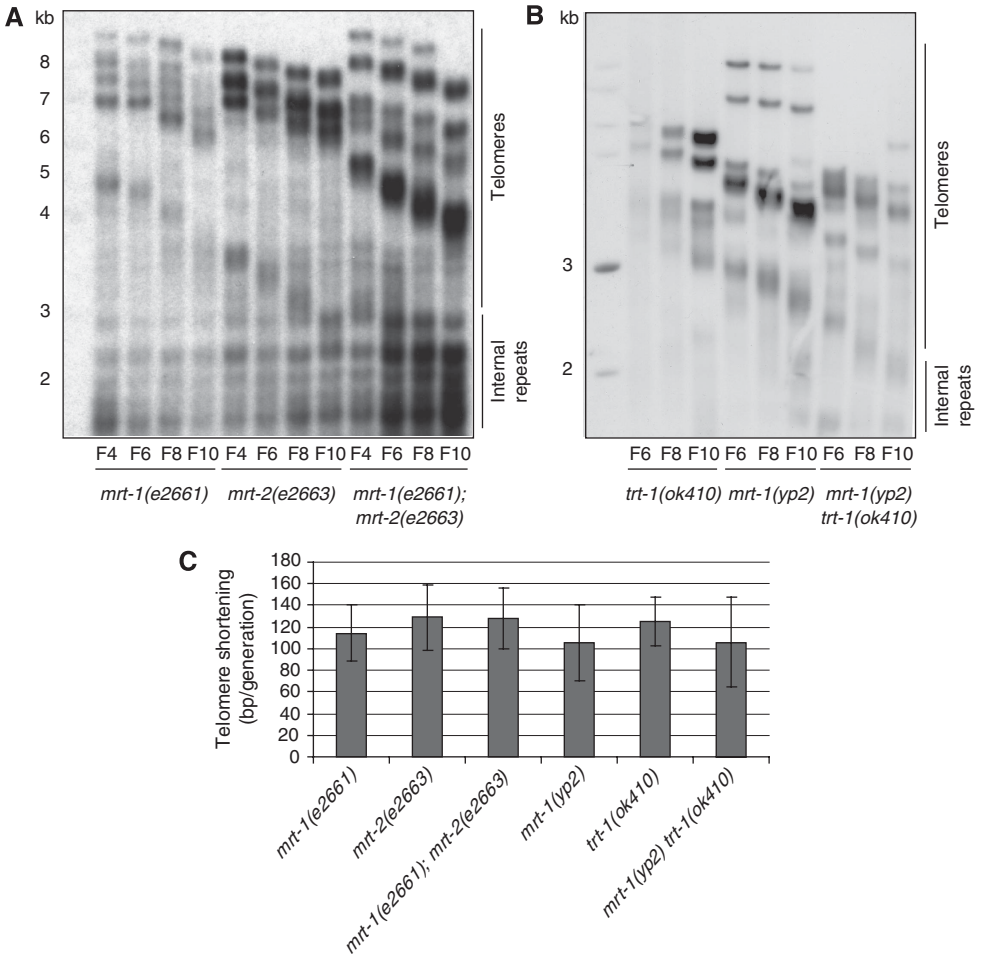

Figure 5 *mrt-1*, *mrt-2* and *trt-1* function in the same genetic pathway. (**A**, **B**) Southern blots of various *mrt-1* single and double mutant combinations performed as described for Figure 1A. Internal-repeat signals (Wicky *et al*, 1996) and telomere signals are indicated on the right. (**C**) Statistical analysis of the rate of telomere shortening in single and double mutants. The rate of telomere shortening indicates the mean of individual telomere shortening rate measurements over at least three analysed generations (see Supplementary data) and error bars show standard deviations.

and Cech, 2001; Veldman *et al*, 2004; Hockemeyer *et al*, 2005). For example, human POT1 can facilitate telomerase activity *in vitro* when in a complex with its interacting protein TPP1 (Lei *et al*, 2005; Wang *et al*, 2007; Xin *et al*, 2007). Thus, POT1 OB-fold proteins that interact with single-stranded telomeric DNA may perform a conserved function that enables telomerase to act at chromosome termini *in vivo*. This function is difficult to address *in vivo* in organisms where deficiency for POT1 OB-fold proteins results in acute telomere uncapping and/or end-to-end chromosome fusions (Baumann and Cech, 2001; Veldman *et al*, 2004; Hockemeyer *et al*, 2005). In contrast, viable null alleles of *mrt-1* display telomere-erosion phenotypes that are indistinguishable from those of telomerase reverse transcriptase mutants (Figures 1 and 5 and Supplementary Figure 1).

Insight into the telomerase-promoting function of POT1-like proteins is provided by the H127Y mutation in the MRT-1 OB2-fold that abolishes telomerase-mediated telomere replication and affects a conserved histidine (Figure 2A). This amino acid corresponds to His245 of human POT1, which forms hydrogen bonds with the second and fourth nucleotides from the 3′OH terminus of a telomeric oligonucleotide in a crystal structure, suggesting that it may mediate interaction with the chromosome terminus *in vivo* (Lei *et al*, 2004). Our results demonstrate that this amino acid is required for interaction of MRT-1 with single-stranded DNA *in vitro* and that this residue is essential for *in vivo* telomerase activity. Thus, the DNA-binding activity of POT1-related OB-fold proteins is likely to be critical for telomerase activity *in vivo*.

Our genetic analysis of *mrt-1; mrt-2* double mutants indicates that MRT-1 and the 9-1-1 DNA-damage response complex act together in a single pathway to facilitate telomerase-dependent telomere replication. While *C. elegans* 9-1-1 complex mutants display defects in responding to DSB and ICL lesions, the *mrt-1* alleles (including two probable null alleles) are only deficient for ICL repair. It is intriguing that MRT-1 and MRT-2 function in both telomerase-dependent telomere replication and ICL repair. Although this may be coincidental, we favour the possibility that telomerase-dependent telomere replication and some ICL lesions may share common features. Human SNM1B/Apollo interacts with telomere-binding proteins and is required for telomere function *in vivo* (Freibaum and Counter, 2006, 2008; Lenain *et al*, 2006; van Overbeek and de Lange, 2006; Demuth *et al*, 2008), whereas human SNM1C/Artemis facilitates telomere capping (Rooney *et al*, 2003). This telomere association may

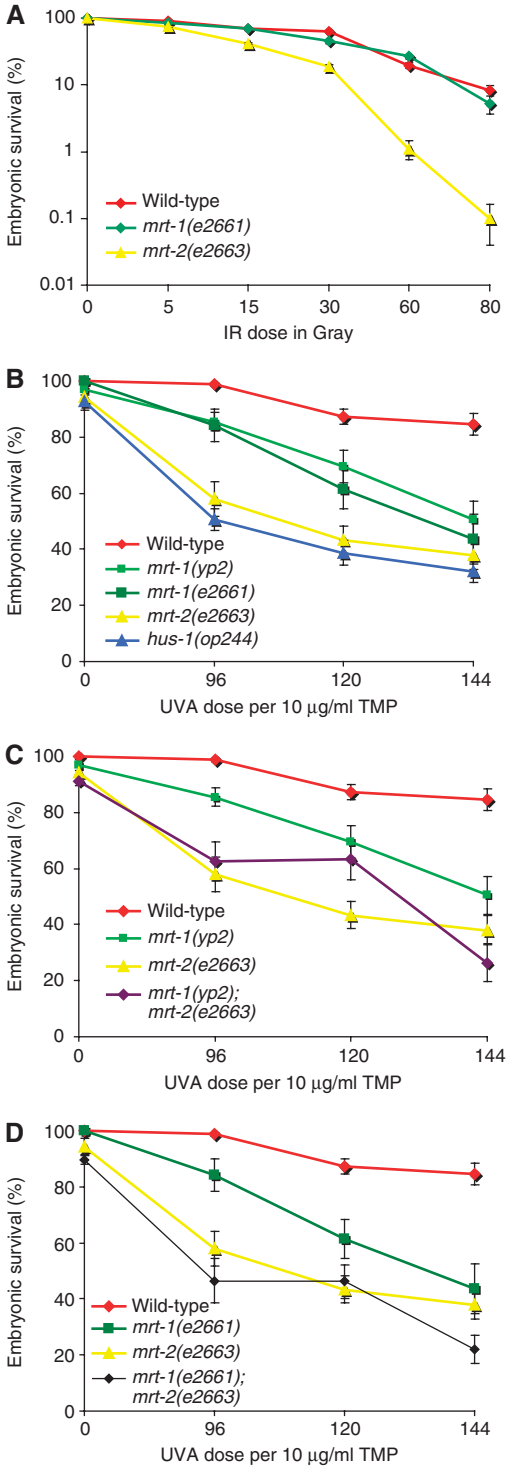

Figure 6 *mrt-1* mutants are hypersensitive to UV/TMP but not to ionizing radiation. (**A**) Sensitivity of wild-type, *mrt-1(e2661)* and *mrt-2(e2663)* strains to increasing doses of ionizing radiation was assayed as described (Ahmed and Hodgkin, 2000). (**B**) Sensitivity of wild-type and *mrt-1(yp2)*, *mrt-1(e2661)*, *mrt-2(e2663)* and *hus-1(op244)* mutants to UV/TMP with 10 μg/ml TMP and the indicated doses of UVA light (bottom) in Joules/cm^2 was assayed as described (Collis *et al*, 2006). (**C**) Sensitivity of wild-type, *mrt-1(yp2)* and *mrt-2(e2663)* in comparison with *mrt-1(yp2)*; *mrt-2(e2663)* double mutants to UV/TMP as described in panel B. (**D**) Sensitivity of wild-type, *mrt-1(e2661)* and *mrt-2(e2663)* in comparison with *mrt-1(e2661)*; *mrt-2(e2663)* double mutants to UV/TMP as described in panel B. (A–D) Results show averages from three independent experiments and error bars represent standard error of the mean for all graphs depicted.

be specific to metazoans, as independent large-scale genetic screens have failed to reveal a role for *S. cerevisiae PSO2/SNM1* in telomere homeostasis (Askree *et al*, 2004; Downey *et al*, 2006). Our results indicate that MRT-1 possesses dual, separable biochemical activities: binding to single-stranded DNA (OB-fold) and nucleolytic processing (SNM1 nuclease domain). These activities are likely to act sequentially *in vivo* and may facilitate both ICL repair and telomere-repeat addition by telomerase, although the role of the nuclease domain of MRT-1 in telomere replication is presently unclear. Given that the mammalian 9-1-1 complex physically interacts with telomerase (Francia *et al*, 2006), and that subunits of this complex, as well as MRT-1, are required for *de novo* telomere repeat addition at *C. elegans* chromosome ends, we favour the possibility that an ancient metazoan DNA-damage response pathway may be triggered at chromosome termini prior to telomere-repeat addition by telomerase.

Secondary DNA structures arising at telomeres, some of which could resemble intermediates formed at ICL lesions, might serve as substrates for MRT-1. At present we can only speculate on the structure of the *in vivo* substrates of MRT-1. Despite evidence that Pso2p/ SNM1 nuclease activity is needed for ICL repair and that Pso2p/ SNM1 acts downstream of the initial cleavage event at a cross-link lesion, the relevant *in vivo* substrates processed by Pso2p are still unknown (Magana-Schwencke *et al*, 1982; Li *et al*, 2005). Of the mammalian homologues, DNA substrates have only been defined for SNM1C/Artemis, which targets hairpin intermediates generated during V(D)J recombination (Rooney *et al*, 2003). It is of interest that the ciliate TEBP β-protein has been implicated in resolution of the telomeric DNA G-quadruplex secondary structure during DNA replication, perhaps coincident with telomerase activity (Paeschke *et al*, 2008). Additional unusual DNA structures at telomeres include (1) the T-loop, where the terminal 3′ overhang folds back to form a structure that resembles a recombination intermediate, (2) stalled replication forks that commonly occur at repetitive DNA sequences (Griffith *et al*, 1999; Fouche *et al*, 2006) and (3) simple 3′ overhangs that are ubiquitous telomeric structures and would be excellent substrates for the 3′-to-5′ nuclease activity of MRT-1 (Figure 3 and Supplementary Figure 4). Finally, leading-strand DNA synthesis at chromosome termini has been suggested to yield the preferred substrate of telomerase (Chai *et al*, 2006), and blunt chromosome termini could be a substrate for the nuclease activity of MRT-1. In this case, 5′-to-3′ nuclease activity at blunt chromosome termini would be required to generate a 3′ overhang for telomerase, and MRT-1 did not possess such an activity under our experimental conditions (Figure 3E and F). However, studies of yeast and vertebrate SNM1 homologues of MRT-1 indicate that SNM1 nucleases often display 5′-to-3′ nuclease activity *in vitro* (Li *et al*, 2005; Hejna *et al*, 2007), which raises the possibility that MRT-1 may function analogously to create 3′ overhangs at blunt chromosome termini *in vivo*. Note that telomerase enzymes from various species are associated with a nuclease activity that can remove non-telomeric nucleotides from 3′ ends of primers in *in vitro* telomerase assays (Collins and Greider, 1993; Autexier and Greider, 1994; Cohn and Blackburn, 1995; Melek *et al*, 1996; Bhattacharyya and Blackburn, 1997; Prescott and Blackburn, 1997; Bednenko *et al*, 1997; Greene *et al*, 1998; Lue and Peng, 1998; Niu *et al*, 2000; Huard and

Autexier, 2003, 2004; Oulton and Harrington, 2004), although studies with recombinant telomerase suggest that this nuclease activity may be a property of telomerase itself (Collins and Gandhi, 1998; Huard and Autexier, 2004; Oulton and Harrington, 2004). We conclude that the *C. elegans* ICL repair protein MRT-1 may interact with single-stranded telomeric DNA to promote telomere-repeat addition by telomerase and may function in a nucleolytic processing event at chromosome ends.

Materials and methods

Protein expression and purification

Proteins encoded by pAG472 (6 × His–MBP–TEV–MRT-1), pAG474 (6 × His–MBP–TEV–MRT-1(H127Y), pAG538 (6 × His–MBP–TEV–MRT-1(D245A) and pAG473 (6 × His–MBP–TEV–MRT-1(4mut)) (see Supplementary data) were expressed in *E. coli* BL21(DE3) pRil (Invitrogen). Cultures (500 ml) were induced at OD_{600} ~ 1.0 with 5 μM IPTG and grown overnight at 12°C. Bacteria were lysed in one-pellet volume of lysis buffer (50 mM sodium phosphate, pH 8.0, 300 mM NaCl, 10 mM imidazole, 0.1% Tween, 10% glycerol, protease inhibitor cocktail complete (Roche) and 1 mg/ml lysozyme) by sonication, centrifuged and purified over a TALON metal affinity resin (Clontech) (see Supplementary data). MBP-6 × His–TEV–MRT-1 containing fractions eluted with 120 mM imidazole were cleaved with 6 × His–TEV1 protease at 4°C overnight. Cleavage efficiency was monitored by SDS–PAGE and Coomassie staining. Extracts were adjusted to a final concentration of 40 mM imidazole and incubated with NiNTA agarose (Qiagen) (see Supplementary data). The flow through was collected and assayed for MRT-1 by SDS–PAGE, Coomassie staining and western blotting, dialysed against 50 mM KCl, 20 mM potassium phosphate, pH 8.0, 20% glycerol, 0.2% Tween 20, 5 mM β-mercaptoethanol and concentrated up to 10-fold in an Amicon Ultra Centricon 30K MWCO (Millipore).

Proteins encoded by pAG368 (6 × His–MRT-1) and pAG369 (6 × His–MRT-1(H127Y)) were expressed as described above, but with IPTG induction for 2 h at 25°C. Bacteria were lysed by sonication in one-pellet volume of lysis buffer (20 mM sodium phosphate, pH 8.0, 500 mM NaCl, 20 mM imidazole, 0.2% Tween, 20% glycerol, 5 mM β-mercaptoethanol, protease inhibitor cocktail complete (Roche)) containing 1 mg/ml lysozyme, centrifuged and purified over a NiNTA agarose column (Qiagen) according to manufacturer's instructions. Protein fractions were pooled and then dialysed and concentrated as described above.

Nuclease assay

Radiolabelled oligonucleotide (5 nM) was incubated with 70 nM of cleaved and purified MRT-1 wild-type or mutant protein in a final volume of 10 μl reaction buffer (50 mM Tris–HCl, pH 8.0, 50 mM NaCl, 10 mM $MgCl_2$, 0.5 mM EDTA, 10% glycerol) unless indicated otherwise. Thirty units of RecJf (New England Biolabs) and 5–10 U *Exo*I (New England Biolabs) were used as controls. Reactions were incubated at RT for 1 h unless stated otherwise. An equal volume of formamide buffer (95% formamide, 18 mM EDTA, 0.025% SDS, 0.025% bromphenol blue, 0.025% xylene xyanol) was then added to each sample. Samples were heated at 80°C for 3–5 min and loaded onto a denaturing 12% polyacrylamide gel (40% acrylamide 29:1).

Electrophoretic mobility-shift assay

Radiolabelled oligonucleotide (5 nM) was incubated with 6 × His–MRT1 alleles or TEV-cleaved and dialysed MRT-1 protein versions at the indicated concentrations for 20 min at RT in 25 mM Hepes pH 7.5, 50 mM NaCl, 1 mM EDTA, 5% glycerol, 1 mM DTT in the presence of 100 ng of poly(dI–dC) as nonspecific competitor. For DNA competition experiments, proteins were incubated with a radiolabelled oligonucleotide in the absence of poly(dI–dC) for 20 min at RT. Unlabelled oligonucleotide was then added to the samples followed by incubation for 20 min. Samples were loaded onto a pre-run 6% polyacrylamide (29:1) gel and a marker dye was loaded in parallel into one well. The gel was then run for 3–5 h with 7 V/cm in 0.5 × TBE at 4°C, dried and exposed to film. DNA binding was quantified using Fujifilm FLA-5100 and LAS-4000 scanners and AIDA Image Analyzer v3.27 software (Raytest).

Supplementary data

Supplementary data are available at *The EMBO Journal* Online (http://www.embojournal.org).

Acknowledgements

We thank LinNan Shen and Ron Hay for advice in protein purification; Diego Miranda-Saavreda for help with bioinformatics; Iuval Clejan for help with end-joining experiments; Anne-Cécile Déclais, David Lilley and Zbigniev Dominski for discussing nuclease assays; V Makrantoni, P Ibanez and A Craig for critical reading of the manuscript; the National Bioresource Project for the Experimental Animal *C. elegans* (Shohei Mitani) for *mrt-1(tm1354)* and the Caenorhabditis Genetics Center (CGC) for strains. We are grateful for support from Jonathan Hodgkin, in whose laboratory *mrt-1(e2661)* was isolated and initially characterized by SA. BM and AG were funded by a CR-UK CDA award, LJB and SJB by CR-UK and IC by a UNC Lineberger Comprehensive Cancer Center postdoctoral fellowship. BM, YL and SA were funded by NIH Grant GM066228.

References

Ahmed S, Alpi A, Hengartner MO, Gartner A (2001) *C. elegans* RAD-5/CLK-2 defines a new DNA damage checkpoint protein. *Curr Biol* **11:** 1934–1944

Ahmed S, Hodgkin J (2000) MRT-2 checkpoint protein is required for germline immortality and telomere replication in *C. elegans*. *Nature* **403:** 159–164

Aravind L (1999) An evolutionary classification of the metallo-beta-lactamase fold proteins. *In Silico Biol* **1:** 69–91

Askree SH, Yehuda T, Smolikov S, Gurevich R, Hawk J, Coker C, Krauskopf A, Kupiec M, McEachern MJ (2004) A genome-wide screen for *Saccharomyces cerevisiae* deletion mutants that affect telomere length. *Proc Natl Acad Sci USA* **101:** 8658–8663

Autexier C, Greider CW (1994) Functional reconstitution of wild-type and mutant *Tetrahymena* telomerase. *Genes Dev* **8:** 563–575

Bae JB, Mukhopadhyay SS, Liu L, Zhang N, Tan J, Akhter S, Liu X, Shen X, Li L, Legerski RJ (2008) Snm1B/Apollo mediates replication fork collapse and S phase checkpoint activation in response to DNA interstrand cross-links. *Oncogene* **27:** 5045–5056

Baumann P, Cech TR (2001) Pot1, the putative telomere end-binding protein in fission yeast and humans. *Science* **292:** 1171–1175

Bednenko J, Melek M, Greene EC, Shippen DE (1997) Developmentally regulated initiation of DNA synthesis by telomerase: evidence for factor-assisted *de novo* telomere formation. *EMBO J* **16:** 2507–2518

Bhattacharyya A, Blackburn EH (1997) A functional telomerase RNA swap *in vivo* reveals the importance of nontemplate RNA domains. *Proc Natl Acad Sci USA* **94:** 2823–2827

Boerckel J, Walker D, Ahmed S (2007) The *Caenorhabditis elegans* Rad17 homolog HPR-17 is required for telomere replication. *Genetics* **176:** 703–709

Callebaut I, Moshous D, Mornon JP, de Villartay JP (2002) Metallo-beta-lactamase fold within nucleic acids processing enzymes: the beta-CASP family. *Nucleic Acids Res* **30:** 3592–3601

Carfi A, Pares S, Duee E, Galleni M, Duez C, Frere JM, Dideberg O (1995) The 3D structure of a zinc metallo-beta-lactamase from *Bacillus cereus* reveals a new type of protein fold. *EMBO J* **14:** 4914–4921

Chai W, Du Q, Shay JW, Wright WE (2006) Human telomeres have different overhang sizes at leading versus lagging strands. *Mol Cell* **21:** 427–435

Clejan I, Boerckel J, Ahmed S (2006) Developmental modulation of nonhomologous end joining in *Caenorhabditis elegans*. *Genetics* **173:** 1301–1317

Cohn M, Blackburn EH (1995) Telomerase in yeast. *Science* **269:** 396–400

Collins K (2006) The biogenesis and regulation of telomerase holoenzymes. *Nat Rev Mol Cell Biol* **7:** 484–494

Collins K, Greider CW (1993) *Tetrahymena* telomerase catalyzes nucleolytic cleavage and nonprocessive elongation. *Genes Dev* **7:** 1364–1376

Collins K, Gandhi L (1998) The reverse transcriptase component of the *Tetrahymena* telomerase ribonucleoprotein complex. *Proc Natl Acad Sci USA* **95:** 8485–8490

Collis SJ, Barber LJ, Ward JD, Martin JS, Boulton SJ (2006) *C. elegans* FANCD2 responds to replication stress and functions in interstrand cross-link repair. *DNA Repair (Amst)* **5:** 1398–1406

d'Adda di Fagagna F, Teo SH, Jackson SP (2004) Functional links between telomeres and proteins of the DNA-damage response. *Genes Dev* **18:** 1781–1799

Demuth I, Bradshaw PS, Lindner A, Anders M, Heinrich S, Kallenbach J, Schmelz K, Digweed M, Meyn MS, Concannon P (2008) Endogenous hSNM1B/Apollo interacts with TRF2 and stimulates ATM in response to ionizing radiation. *DNA Repair (Amst)* **7:** 1192–1201

Demuth I, Digweed M, Concannon P (2004) Human SNM1B is required for normal cellular response to both DNA interstrand crosslink-inducing agents and ionizing radiation. *Oncogene* **23:** 8611–8618

Dominski Z (2007) Nucleases of the metallo-beta-lactamase family and their role in DNA and RNA metabolism. *Crit Rev Biochem Mol Biol* **42:** 67–93

Downey M, Houlsworth R, Maringele L, Rollie A, Brehme M, Galicia S, Guillard S, Partington M, Zubko MK, Krogan NJ, Emili A, Greenblatt JF, Harrington L, Lydall D, Durocher D (2006) A genome-wide screen identifies the evolutionarily conserved KEOPS complex as a telomere regulator. *Cell* **124:** 1155–1168

Dronkert ML, de Wit J, Boeve M, Vasconcelos ML, van Steeg H, Tan TL, Hoeijmakers JH, Kanaar R (2000) Disruption of mouse SNM1 causes increased sensitivity to the DNA interstrand cross-linking agent mitomycin C. *Mol Cell Biol* **20:** 4553–4561

Fouche N, Ozgur S, Roy D, Griffith JD (2006) Replication fork regression in repetitive DNAs. *Nucleic Acids Res* **34:** 6044–6050

Francia S, Weiss RS, Hande MP, Freire R, d'Adda di Fagagna F (2006) Telomere and telomerase modulation by the mammalian Rad9/Rad1/Hus1 DNA-damage-checkpoint complex. *Curr Biol* **16:** 1551–1558

Freibaum BD, Counter CM (2006) hSnm1B is a novel telomere-associated protein. *J Biol Chem* **281:** 15033–15036

Freibaum BD, Counter CM (2008) The protein hSnm1B is stabilized when bound to the telomere-binding protein TRF2. *J Biol Chem* **283:** 23671–23676

Fu D, Collins K (2007) Purification of human telomerase complexes identifies factors involved in telomerase biogenesis and telomere length regulation. *Mol Cell* **28:** 773–785

Garcia CK, Wright WE, Shay JW (2007) Human diseases of telomerase dysfunction: insights into tissue aging. *Nucleic Acids Res* **35:** 7406–7416

Gengyo-Ando K, Mitani S (2000) Characterization of mutations induced by ethyl methanesulfonate, UV, and trimethylpsoralen in the nematode *Caenorhabditis elegans*. *Biochem Biophys Res Commun* **269:** 64–69

Greene EC, Bednenko J, Shippen DE (1998) Flexible positioning of the telomerase-associated nuclease leads to preferential elimination of nontelomeric DNA. *Mol Cell Biol* **18:** 1544–1552

Greider CW, Blackburn EH (1989) A telomeric sequence in the RNA of *Tetrahymena* telomerase required for telomere repeat synthesis. *Nature* **337:** 331–337

Griffith JD, Comeau L, Rosenfield S, Stansel RM, Bianchi A, Moss H, de Lange T (1999) Mammalian telomeres end in a large duplex loop. *Cell* **97:** 503–514

Hazrati A, Ramis-Castelltort M, Sarkar S, Barber LJ, Schofield CJ, Hartley JA, McHugh PJ (2008) Human SNM1A suppresses the DNA repair defects of yeast pso2 mutants. *DNA Repair (Amst)* **7:** 230–238

Hejna J, Philip S, Ott J, Faulkner C, Moses R (2007) The hSNM1 protein is a DNA 5′-exonuclease. *Nucleic Acids Res* **35:** 6115–6123

Hemphill AW, Bruun D, Thrun L, Akkari Y, Torimaru Y, Hejna K, Jakobs PM, Hejna J, Jones S, Olson SB, Moses RE (2008) Mammalian SNM1 is required for genome stability. *Mol Genet Metab* **94:** 38–45

Henriques JA, Moustacchi E (1980) Isolation and characterization of pso mutants sensitive to photo-addition of psoralen derivatives in *Saccharomyces cerevisiae*. *Genetics* **95:** 273–288

Hockemeyer D, Sfeir AJ, Shay JW, Wright WE, de Lange T (2005) POT1 protects telomeres from a transient DNA damage response and determines how human chromosomes end. *EMBO J* **24:** 2667–2678

Hofmann ER, Milstein S, Boulton SJ, Ye M, Hofmann JJ, Stergiou L, Gartner A, Vidal M, Hengartner MO (2002) *Caenorhabditis elegans* HUS-1 is a DNA damage checkpoint protein required for genome stability and EGL-1-mediated apoptosis. *Curr Biol* **12:** 1908–1918

Horvath MP, Schweiker VL, Bevilacqua JM, Ruggles JA, Schultz SC (1998) Crystal structure of the *Oxytricha nova* telomere end binding protein complexed with single strand DNA. *Cell* **95:** 963–974

Huard S, Autexier C (2003) The C terminus of the human telomerase reverse transcriptase is a determinant of enzyme processivity. *Nucleic Acids Res* **31:** 4059–4070

Huard S, Autexier C (2004) Human telomerase catalyzes nucleolytic primer cleavage. *Nucleic Acids Res* **32:** 2171–2180

Jeggo PA, Lobrich M (2005) Artemis links ATM to double strand break rejoining. *Cell Cycle* **4:** 359–362

Lei M, Podell ER, Baumann P, Cech TR (2003) DNA self-recognition in the structure of Pot1 bound to telomeric single-stranded DNA. *Nature* **426:** 198–203

Lei M, Podell ER, Cech TR (2004) Structure of human POT1 bound to telomeric single-stranded DNA provides a model for chromosome end-protection. *Nat Struct Mol Biol* **11:** 1223–1229

Lei M, Zaug AJ, Podell ER, Cech TR (2005) Switching human telomerase on and off with hPOT1 protein *in vitro*. *J Biol Chem* **280:** 20449–20456

Lenain C, Bauwens S, Amiard S, Brunori M, Giraud-Panis MJ, Gilson E (2006) The Apollo 5′ exonuclease functions together with TRF2 to protect telomeres from DNA repair. *Curr Biol* **16:** 1303–1310

Li X, Hejna J, Moses RE (2005) The yeast Snm1 protein is a DNA 5′-exonuclease. *DNA Repair (Amst)* **4:** 163–170

Li X, Moses RE (2003) The beta-lactamase motif in Snm1 is required for repair of DNA double-strand breaks caused by interstrand crosslinks in *S. cerevisiae*. *DNA Repair (Amst)* **2:** 121–129

Lowden MR, Meier B, Lee TW, Hall J, Ahmed S (2008) End joining at *Caenorhabditis elegans* telomeres. *Genetics* **180:** 741–754

Lue NF, Peng Y (1998) Negative regulation of yeast telomerase activity through an interaction with an upstream region of the DNA primer. *Nucleic Acids Res* **26:** 1487–1494

Magana-Schwencke N, Henriques JA, Chanet R, Moustacchi E (1982) The fate of 8-methoxypsoralen photoinduced crosslinks in nuclear and mitochondrial yeast DNA: comparison of wild-type and repair-deficient strains. *Proc Natl Acad Sci USA* **79:** 1722–1726

Meier B, Clejan I, Liu Y, Lowden M, Gartner A, Hodgkin J, Ahmed S (2006) trt-1 is the *Caenorhabditis elegans* catalytic subunit of telomerase. *PLoS Genet* **2:** e18

Melek M, Greene EC, Shippen DE (1996) Processing of nontelomeric 3′ ends by telomerase: default template alignment and endonucleolytic cleavage. *Mol Cell Biol* **16:** 3437–3445

Naito T, Matsuura A, Ishikawa F (1998) Circular chromosome formation in a fission yeast mutant defective in two ATM homologues. *Nat Genet* **20:** 203–206

Niu H, Xia J, Lue NF (2000) Characterization of the interaction between the nuclease and reverse transcriptase activity of the yeast telomerase complex. *Mol Cell Biol* **20:** 6806–6815

Nakamura TM, Moser BA, Russell P (2002) Telomere binding of checkpoint sensor and DNA repair proteins contributes to maintenance of functional fission yeast telomeres. *Genetics* **161:** 1437–1452

Niegemann E, Brendel M (1994) A single amino acid change in SNM1-encoded protein leads to thermoconditional deficiency for

DNA cross-link repair in *Saccharomyces cerevisiae*. *Mutat Res* **315:** 275–279

Oulton R, Harrington L (2004) A human telomerase-associated nuclease. *Mol Biol Cell* **15:** 3244–3256

Paeschke K, Juranek S, Simonsson T, Hempel A, Rhodes D, Lipps HJ (2008) Telomerase recruitment by the telomere end binding protein-beta facilitates G-quadruplex DNA unfolding in ciliates. *Nat Struct Mol Biol* **15:** 598–604

Pannicke U, Ma Y, Hopfner KP, Niewolik D, Lieber MR, Schwarz K (2004) Functional and biochemical dissection of the structure-specific nuclease ARTEMIS. *EMBO J* **23:** 1987–1997

Poinsignon C, Moshous D, Callebaut I, de Chasseval R, Villey I, de Villartay JP (2004) The metallo-beta-lactamase/beta-CASP domain of Artemis constitutes the catalytic core for V(D)J recombination. *J Exp Med* **199:** 315–321

Prescott J, Blackburn EH (1997) Telomerase RNA mutations in *Saccharomyces cerevisiae* alter telomerase action and reveal non-processivity *in vivo* and *in vitro*. *Genes Dev* **11:** 528–540

Raices M, Verdun RE, Compton SA, Haggblom CI, Griffith JD, Dillin A, Karlseder J (2008) *C. elegans* telomeres contain G-strand and C-strand overhangs that are bound by distinct proteins. *Cell* **132:** 745–757

Richie CT, Peterson C, Lu T, Hittelman WN, Carpenter PB, Legerski RJ (2002) hSnm1 colocalizes and physically associates with 53BP1 before and after DNA damage. *Mol Cell Biol* **22:** 8635–8647

Ritchie KB, Mallory JC, Petes TD (1999) Interactions of TLC1 (which encodes the RNA subunit of telomerase), TEL1, and MEC1 in regulating telomere length in the yeast *Saccharomyces cerevisiae*. *Mol Cell Biol* **19:** 6065–6075

Rooney S, Alt FW, Lombard D, Whitlow S, Eckersdorff M, Fleming J, Fugmann S, Ferguson DO, Schatz DG, Sekiguchi J (2003) Defective DNA repair and increased genomic instability in Artemis-deficient murine cells. *J Exp Med* **197:** 553–565

Shakirov EV, Surovtseva YV, Osbun N, Shippen DE (2005) The *Arabidopsis* Pot1 and Pot2 proteins function in telomere length homeostasis and chromosome end protection. *Mol Cell Biol* **25:** 7725–7733

Surovtseva YV, Shakirov EV, Vespa L, Osbun N, Song X, Shippen DE (2007) *Arabidopsis* POT1 associates with the telomerase RNP and is required for telomere maintenance. *EMBO J* **26:** 3653–3661

Theobald DL, Wuttke DS (2004) Prediction of multiple tandem OB-fold domains in telomere end-binding proteins Pot1 and Cdc13. *Structure* **12:** 1877–1879

van Overbeek M, de Lange T (2006) Apollo, an Artemis-related nuclease, interacts with TRF2 and protects human telomeres in S phase. *Curr Biol* **16:** 1295–1302

Veldman T, Etheridge KT, Counter CM (2004) Loss of hPot1 function leads to telomere instability and a cut-like phenotype. *Curr Biol* **14:** 2264–2270

Venteicher AS, Meng Z, Mason PJ, Veenstra TD, Artandi SE (2008) Identification of ATPases pontin and reptin as telomerase components essential for holoenzyme assembly. *Cell* **132:** 945–957

Vulliamy TJ, Dokal I (2008) Dyskeratosis congenita: the diverse clinical presentation of mutations in the telomerase complex. *Biochimie* **90:** 122–130

Wang F, Podell ER, Zaug AJ, Yang Y, Baciu P, Cech TR, Lei M (2007) The POT1–TPP1 telomere complex is a telomerase processivity factor. *Nature* **445:** 506–510

Wicky C, Villeneuve AM, Lauper N, Codourey L, Tobler H, Muller F (1996) Telomeric repeats (TTAGGC)n are sufficient for chromosome capping function in *Caenorhabditis elegans*. *Proc Natl Acad Sci USA* **93:** 8983–8988

Xin H, Liu D, Wan M, Safari A, Kim H, Sun W, O'Connor MS, Songyang Z (2007) TPP1 is a homologue of ciliate TEBP-beta and interacts with POT1 to recruit telomerase. *Nature* **445:** 559–562